Spin transition characteristics of molecular solvates of Cu^{II} complexes with nitroxides: sensitivity to the packing type*

N. A. Artiukhova,[a,b]★ G. V. Romanenko,[a] G. A. Letyagin,[a,b] A. S. Bogomyakov,[a,b] S. E. Tolstikov,[a] and V. I. Ovcharenko[a]

[a]*International Tomography Center, Russian Academy of Sciences, 3a ul. Institutskaya, 630090 Novosibirsk, Russian Federation. E-mail: Natalya.artyukhova@tomo.nsc.ru*
[b]*Novosibirsk State University, 2 ul. Pirogova, 630090 Novosibirsk, Russian Federation*

A method for the synthesis of solvates of dinuclear heterospin complexes of bis(hexafluoroacetylacetonato)copper(II) with 2-(4-methylpyridin-3-yl)-4,4,5,5-tetramethyl-4,5-dihydro-1*H*-imidazole-3-oxide-1-oxyl (L^{Me}) and 2-(4-ethylpyridin-3-yl)-4,4,5,5-tetramethyl-4,5-dihydro-1*H*-imidazole-3-oxide-1-oxyl (L^{Et}) of the composition $[Cu(hfac)_2L^R]_2 \cdot Solv$ (Solv = benzene, bromobenzene, toluene, *o*-xylene, *p*-xylene) was developed. It was found that a decrease in temperature induces structural transformations of the solid phases of the complexes followed by significant changes in the distances between the paramagnetic centers in the intramolecular exchange clusters $\{Cu^{2+}—O^{\bullet}—\}$ from 2.321 to 1.974 Å. As a result, the temperature dependences of the effective magnetic moment $\mu_{eff}(T)$ exhibit magnetic features similar to spin transitions. An analysis of the shape of the $\mu_{eff}(T)$ curves suggested that the magnetic properties of the compounds under study depend primarily on the molecular packing. A comparison of the magneto-structural correlations typical of the $[Cu(hfac)_2L^R]_2 \cdot Solv$ complexes studied in this work with the data obtained earlier for analogous solvates of heterospin polymer chain complexes showed that the spin transition characteristics of the $[Cu(hfac)_2L^R]_2 \cdot Solv$ systems are much less sensitive to the change of the solvent than the corresponding characteristics of the heterospin polymers containing solvate molecules in the interchain space. The magnetic characteristics of the heterospin dimer molecules depend primarily on which cavity between the dimers is filled with solvate molecules. For solvates with monoclinic symmetry, changes in the solvent molecules occupying same-type cavities have almost no effect on the spin transition characteristics in the heterospin exchange cluster.

Key words: Cu^{II} complexes, hexafluoroacetylacetonates, nitroxide radicals, phase transitions, thermomagnetic measurements, X-ray diffraction analysis, magneto-structural correlations, solvates.

The solid phases of heterospin complexes based on bis(hexafluoroacetylacetonato)copper(II) $[Cu(hfac)_2]$ with nitronyl nitroxide radicals attract the interest of researchers due to the fact that they can undergo structural transformations accompanied by spin transitions under the action of external factors.[1,2] It was found that in these multispin compounds called breathing crystals,[3—5] even minor changes in the structure of the paramagnetic ligand cause significant changes in the shape of the temperature dependence of the effective magnetic moment $\mu_{eff}(T)$. By considering polymer chain heterospin complexes of $[Cu(hfac)_2]$ with pyrazolyl-substituted nitroxides capable of incorporating solvent molecules into the interchain space, it was shown that the characteristics of the magnetic anomalies can be changed with ease by varying the nature of solvate molecules.[6—8]

We synthesized a few series of solvates of dinuclear heterospin complexes of $[Cu(hfac)_2]$ with the nitronyl nitroxide radicals L^{Me} and L^{Et} of the composition $[Cu(hfac)_2L^R]_2 \cdot Solv$. The solid phases of these solvates have the molecular structure. Temperature changes induce significant structural transformations of these complexes, leading to considerable (from 2.321 to 1.974 Å) changes in the distances between the paramagnetic centers (PMC), *viz.*, Cu^{2+} ions and nitroxide O atoms (O_{NO}), which are responsible for the appearance of features (anomalies) in the $\mu_{eff}(T)$ dependences. We established correlations between the temperature-induced changes in the magnetic properties and the structure of the compounds and showed that the spin transition characteristics of the solvates of heterospin molecular complexes are more sensitive to the packing type (*i.e.*, mutual arrangement of paramagnetic

* Based on the Materials of the Russian National Cluster of Conferences on Inorganic Chemistry "InorgChem-2018" (September 17—21, 2018, Astrakhan, Russia).

Published in Russian in *Izvestiya Akademii Nauk. Seriya Khimicheskaya,* No. 4, pp. 0732—0742, April, 2019.

molecules of the heterospin complex and diamagnetic solvent molecules in the solid phase) rather than to the nature of the solvent molecules. Besides, among all the $[Cu(hfac)_2L^R]_2 \cdot Solv$ complexes studied, those with the same packing type exhibit similar $\mu_{eff}(T)$ dependences irrespective of substituents in the nitronyl nitroxide radicals. This fundamentally distinguishes these compounds from the previously studied solvates of polymer chain heterospin complexes of $Cu(hfac)_2$ with spin-labeled pyrazoles whose magnetic properties are highly sensitive not only to the nature and molecular geometry of solvents, but also to any changes in the structure of paramagnetic ligands.[6—8]

Experimental

2-(4-Methylpyridin-3-yl)-4,4,5,5-tetramethyl-4,5-dihydro-1*H*-imidazole-3-oxide-1-oxyl (L^{Me}),[9] 4-ethylnicotinaldehyde,[10] 2,3-bishydroxylamino-2,3-dimethylbutane,[11] and bis(hexafluoroacetylacetonato)copper(II) ($Cu(hfac)_2$)[12] were obtained following known procedures; commercially available reagents and solvents were used as received.

TLC monitoring was performed using Macherey-Nagel Silica Gel 60 F_{254} aluminum sheets (Germany) and Merck silica gel (0.063—0.200 mm) for column chromatography. Melting points were determined on a Stuart melting point apparatus. Elemental analyses (C, H, and N) were carried out with a EURO EA3000 elemental analyzer (EuroVector, Italy) using partially desolvated samples.

The magnetic susceptibility of polycrystalline samples was measured using a Quantum Design MPMS*XL* SQUID magnetometer (USA) in the temperature range from 2 to 300 K in a magnetic field of 5 kOe. The paramagnetic components of the magnetic susceptibility χ were determined taking into account the diamagnetic contribution which was estimated from the Pascal constants. The effective magnetic moment at different temperatures was calculated using the expression

$$\mu_{eff}(T) = (3k/N\mu_B{}^2 \cdot \chi T)^{1/2} \approx (8\chi T)^{1/2},$$

where N, k, and μ_B are the Avogadro constant, Boltzmann constant, and Bohr magneton, respectively.

X-Ray diffraction study. X-Ray diffraction data from single crystals were collected on a Bruker SMART APEX II diffractometer (Germany, Mo-Kα radiation) equipped with a Helix low-temperature accessory (Oxford Cryosystems, United Kingdom) and on a Bruker APEX DUO diffractometer (Cu-Kα radiation). The absorption corrections were applied using the Bruker SADABS software, v. 2.10. The structures were solved by the direct methods and refined by the full-matrix least squares method with anisotropic displacement parameters for all non-hydrogen atoms. The hydrogen atoms were positioned geometrically and refined using the riding model. The phase transition of $[Cu(hfac)_2L^{Et}]_2 \cdot o$-Xyl crystals occurs with the formation of a superstructure, which manifests itself in 12-fold increase in the unit cell volume. This structure was solved with an admissible R-factor value only using the data set obtained at 105 K. All calculations and structure refinement were carried out using the Bruker Shelxtl Version 6.14 software. Crystallographic data for the compounds studied and their refcodes in the Cambridge Structural Database[13] are presented in Tables 1—4, while selected bond lengths and bond angles are listed in Tables 5—7.

The CIF files containing complete information on the structures studied were deposited with the Cambridge Structural Database at www.ccdc.cam.ac.uk/data_request/cif.

2-(4-Ethylpydin-3-yl)-4,4,5,5-tetramethyl-4,5-dihydro-1*H*-imidazole-3-oxide-1-oxyl (L^{Et}). To a solution of 2,3-bis(hydroxylamino)-2,3-dimethylbutane (0.244 g, 1 mmol) in MeOH (3 mL), 4-ethylnicotinaldehyde (0.135 g, 1 mmol) was added at room temperature. The reaction mixture was stirred for 48 h at room temperature and then kept for 24 h at 4 °C. The residue that formed was filtered off, washed on the filter with MeOH, and dried in a vacuum oven. 2-(4-Ethylpydin-3-yl)-4,4,5,5-tetramethyl-4,5-dihydro-1*H*-imidazole (0.250 g) was obtained as white powder which was then used without additional purification. To a suspension of 2-(4-ethylpydin-3-yl)-4,4,5,5-tetramethyl-4,5-dihydro-1*H*-imidazole in MeOH (3 mL), MnO_2 (1 g) was added on cooling on a water bath and the mixture was stirred for 1 h. The solution was filtered, the residue was washed with MeOH, and the combined filtrate was concentrated. The residue was dissolved in EtOAc, filtered through a SiO_2 layer (2×5 cm), and the eluate was concentrated on a rotary evaporator. The product was recrystallized from a CH_2Cl_2—hexane mixture, the solution was kept at 4 °C. The yield was 0.150 g (40%), purple prismatic crystals. M.p. 90—92 °C (decomp.). Found (%): C, 63.1; H, 7.5; N, 16.0. $C_{13}H_{18}N_3O_2$. Calculated (%): C, 62.9; H, 7.3; N, 16.9.

Tetrakis(1,1,1,5,5,5-hexafluoro-2,4-pentanedionato-*O,O'*)-bis[μ_2-2-(4-methylpyridin-3-yl)-4,4,5,5-tetramethyl-4,5-dihydro-1*H*-imidazole-3-oxide-1-oxyl]dicopper(II) benzene solvate, $[Cu(hfac)_2L^{Me}]_2 \cdot PhH$, from this point on **1 · PhH.** To a solution of $Cu(hfac)_2$ (0.039 g, 0.082 mmol) and L^{Me} (0.020 g, 0.082 mmol) in CH_2Cl_2 (1 mL), benzene (2 mL) was added and the mixture was allowed to stand in an open vessel for 24 h at 4 °C. Bulky red-brown prismatic crystals that formed were filtered off, washed with cold hexane, and dried in air. The yield was 35 mg (60%). Found (%): C, 41.7; H, 3.5; F, 28.3; N, 5.5. $C_{52}H_{46}Cu_2F_{24}N_6O_{12}$. Calculated (%): C, 40.9; H, 3.0; F, 29.8; N, 5.5.

Complexes $[Cu(hfac)_2L^{Me}]_2 \cdot PhMe$ and $[Cu(hfac)_2L^{Me}]_2 \cdot o$-Xyl were obtained analogously to $[Cu(hfac)_2L^{Me}]_2 \cdot PhH$ using toluene and *o*-xylene as respective solvents.

Tetrakis(1,1,1,5,5,5-hexafluoro-2,4-pentanedionato-*O,O'*)-bis[μ_2-2-(4-methylpyridin-3-yl)-4,4,5,5-tetramethyl-4,5-dihydro-1*H*-imidazole-3-oxide-1-oxyl]dicopper(II) toluene solvate, $[Cu(hfac)_2L^{Me}]_2 \cdot PhMe$, from this point on **1 · PhMe**, yield 65%, bulky dark-red prismatic crystals. Found (%): C, 40.7; H, 3.0; F, 29.3; N, 5.5. $C_{53}H_{48}Cu_2F_{24}N_6O_{12}$. Calculated (%): C, 41.3; H, 3.1; F, 29.6; N, 5.5.

Tetrakis(1,1,1,5,5,5-hexafluoro-2,4-pentanedionato-*O,O'*)-bis[μ_2-2-(4-methylpyridin-3-yl)-4,4,5,5-tetramethyl-4,5-dihydro-1*H*-imidazole-3-oxide-1-oxyl]dicopper(II) *o*-xylene solvate, $[Cu(hfac)_2L^{Me}]_2 \cdot o$-Xyl, from this point on **1 · *o*-Xyl**, yield 80%, bulky dark-red prismatic crystals. Found (%): C, 39.3; H, 3.0; F, 26.9; N, 5.4. $C_{54}H_{50}Cu_2F_{24}N_6O_{12}$. Calculated (%): C, 41.7; H, 3.2; F, 29.3; N, 5.4.

Tetrakis(1,1,1,5,5,5-hexafluoro-2,4-pentanedionato-*O,O'*)-bis[μ_2-2-(4-ethylpydin-3-yl)-4,4,5,5-tetramethyl-4,5-dihydro-1*H*-imidazole-3-oxide-1-oxyl]dicopper(II) benzene solvate, $[Cu(hfac)_2L^{Et}]_2 \cdot PhH$, from this point on **2 · PhH.** To a solution of $Cu(hfac)_2$ (0.036 g, 0.075 mmol) and L^{Et} (0.020 g, 0.075 mmol) in CH_2Cl_2 (1 mL), benzene (2 mL) was added and the mixture was allowed to stand in an open vessel for 24 h at 4 °C. Red-brown

Table 1. Crystallographic data, X-ray diffraction data, and refinement statistics for solvated complexes **1**·Solv (Solv = PhH, PhMe, *o*-Xyl)

Parameter	**1**·PhH				**1**·PhMe			**1**·*o*-Xyl		
T/K	320	295	220	125	295	240	175	110	295	125
Space group	$P2_1/c$				$P2_1/c$			$P2_1/c$		
Z	2				2			2		
a/Å	13.0409(4)	13.0367(3)	13.0077(5)	12.9396(5)	13.0080(8)	12.9897(8)	12.938(2)	12.900(2)	13.064(3)	12.9554(3)
b/Å	11.3940(4)	11.3550(2)	11.3005(4)	11.2440(5)	11.5631(8)	11.5312(8)	11.496(2)	11.447(2)	11.518(2)	11.4479(2)
c/Å	22.3277(7)	22.2540(5)	22.1370(8)	22.0193(9)	22.3879(14)	22.2855(15)	22.232(4)	22.053(4)	22.554(5)	22.1419(4)
β/deg	102.229(1)	102.416(1)	103.536(2)	105.275(2)	102.840(3)	103.258(3)	104.423(6)	105.262(5)	101.28(3)	103.161(1)
V/Å^3	3242.35(18)	3217.2(1)	3163.6(2)	3090.5(2)	3283.2(4)	3249.1(4)	3202.5(10)	3141.7(9)	3328.1(11)	3197.66(11)
d_{calc}/g cm^{-3}	1.567	1.579	1.606	1.644	1.562	1.578	1.601	1.632	1.555	1.618
θ_{max}/deg	67.797	28.31	67.559	67.620	28.305	67.519	67.477	67.481	28.52	67.671
Number of reflections										
measured	37798	26364	13448	23442	30742	27045	22926	27413	29475	25788
unique	5823	7966	5066	5509	8120	5770	5155	5563	8196	5683
R_{int}	0.0386	0.0840	0.0358	0.0296	0.0752	0.0318	0.0403	0.1037	0.1333	0.0308
I_{hkl} ($I > 2\sigma(I)$)	4743	3579	4199	5041	3404	5319	4716	5299	1834	5141
N	542	551	542	466	553	513	479	487	524	539
GOOF	1.047	0.809	1.142	1.048	0.825	1.027	1.025	1.066	0.606	1.050
$I > 2\sigma(I)$										
R_1	0.0436	0.0419	0.0623	0.0336	0.0493	0.0535	0.0637	0.05559	0.0481	0.0379
wR_2	0.1235	0.0925	0.2023	0.0875	0.1140	0.1420	0.1555	0.1460	0.1101	0.0976
All I_{hkl}										
R_1	0.0526	0.1082	0.0714	0.0370	0.1313	0.0562	0.0706	0.0604	0.2522	0.0423
wR_2	0.1320	0.1095	0.2086	0.0902	0.1371	0.1444	0.1656	0.1681	0.1738	0.1008
CCDC	1872709	1872712	1872714	1872702	1872686	1872698	1872706	1872690	1872716	1872703

Table 2. Crystallographic data, X-ray diffraction data, and refinement statistics for solvated complexes **2**·Solv (Solv = PhH, PhMe)

Parameter	**2**·PhH				**2**·PhMe				
T/K	295	240	200	125	295	240	200	150	105
Space group	$P\bar{1}$				$P\bar{1}$				
Z	1				1				
a/Å	11.7611(4)	11.5719(6)	11.4582(5)	11.3142(4)	11.7995(2)	11.6812(5)	11.6150(7)	11.4381(18)	11.339(2)
b/Å	12.4079(4)	12.3503(6)	12.3270(5)	12.2863(5)	12.5519(2)	12.5060(5)	12.4859(8)	12.6317(19)	12.665(3)
c/Å	14.3303(4)	14.1578(7)	14.0303(6)	13.8868(5)	14.3987(2)	14.3317(6)	14.2920(9)	14.136(2)	14.067(3)
α/deg	67.179(2)	67.9277(14)	68.333(2)	68.7938(14)	66.8940(10)	67.0802(14)	67.2115(18)	67.519(4)	67.673(6)
β/deg	72.101(2)	73.6583(15)	74.780(2)	75.8842(15)	71.8740(10)	71.7160(15)	71.6975(19)	72.233(5)	72.335(6)
γ/deg	65.815(2)	66.3047(14)	66.549(2)	66.7929(15)	65.7680(10)	65.9304(14)	65.9698(19)	65.496(4)	65.345(6)
V/Å^3	1730.73(10)	1696.63(15)	1673.98(13)	1642.45(11)	1759.79(5)	1730.56(13)	1714.94(19)	1691.0(5)	1673.0(6)
d_{calc}/g cm^{-3}	1.570	1.601	1.623	1.654	1.570	1.597	1.611	1.634	1.652
θ_{max}/deg	29.101	67.760	67.513	67.656	29.773	67.586	67.540	67.671	67.689
Number of reflections									
measured	28834	24936	18993	46445	35255	25359	29048	26205	22164
unique	8979	6050	5896	5860	9880	6162	6105	5984	5919
R_{int}	0.0646	0.0285	0.0498	0.0403	0.064	0.0237	0.0236	0.0424	0.0285
I_{hkl} ($I > 2\sigma(I)$)	4314	5881	5144	5509	5133	5999	6000	5803	5787
N	523	551	551	550	577	533	533	498	486
GOOF	0.869	1.040	1.049	1.037	0.876	1.045	1.039	1.041	1.080
$I > 2\sigma(I)$)									
R_1	0.0459	0.0379	0.0400	0.0290	0.0417	0.0445	0.0430	0.0468	0.0365
wR_2	0.1049	0.1018	0.1044	0.0782	0.1033	0.1207	0.1131	0.1213	0.0997
All I_{hkl}									
R_1	0.1127	0.0386	0.0465	0.0309	0.0911	0.0452	0.0434	0.0478	0.0374
wR_2	0.1214	0.1024	0.1110	0.0801	0.1235	0.1213	0.1135	0.1227	0.1017
CCDC	1872715	1872710	1872704	1872705	1872687	1872711	1872708	1872713	1872707

Table 3. Crystallographic data, X-ray diffraction data, and refinement statistics for L^{Et} and **2**·Solv (Solv = *o*-Xyl, *p*-Xyl)

Parameter	*o*-Xyl		*p*-Xyl		L^{Et}
T/K	295	105	295	150	295
Space group	$P2_1/n$	$P2_1/c$	$P2_1/n$	$P2_1/n$	$P2_1/n$
Z	2	24	2	2	12
a/Å	12.9932(3)	24.0832(9)	12.8549(5)	12.7136(3)	10.9324(5)
b/Å	11.3805(3)	32.7355(13)	11.6175(4)	11.5203(2)	22.5228(11)
c/Å	24.2415(5)	50.376(2)	23.6799(8)	23.3051(5)	17.5958(9)
β/deg	105.023(1)	99.426(2)	102.552(2)	101.9457(9)	101.9457(9)
V/Å^3	3462.05(14)	39179(3)	3451.9(2)	3339.45(12)	4317.0(4)
d_{calc}/g cm^{-3}	1.522	1.613	1.526	1.557	1.211
θ_{max}/deg	28.31	28.350	28.377	67.700	67.721
Number of reflections					
measured	28909	430654	32550	37541	51533
unique	8562	88449	8559	5959	7701
(R_{int})	(0.0546)	(0.1229)	(0.0781)	(0.0322)	(0.0631)
I_{hkl} ($I > 2\sigma(I)$)	2684	36565	4179	5480	6833
N	605	5422	559	568	515
GOOF	0.737	0.928	0.856	1.025	1.023
$I > 2\sigma(I)$					
R_1	0.0486	0.1054	0.0439	0.0381	0.0601
wR_2	0.1297	0.2094	0.1025	0.0957	0.1894
All I_{hkl}					
R_1	0.1634	0.2343	0.1015	0.0351	0.0640
wR_2	0.1710	0.2537	0.1186	0.0935	0.1944
CCDC	1872717	1872700	1872692	1872699	1872697

Table 4. Crystallographic data, X-ray diffraction data, and refinement statistics for **2**·PhBr

Parameter	Value					
T/K	295	240	175	115	95	91
Space group	$P\bar{1}$	$P\bar{1}$	$P\bar{1}$	$P\bar{1}$	$P\bar{1}$	$P\bar{1}$
Z	1	1	1	1	1	1
a/Å	11.8430(10)	11.7184(5)	11.5890(4)	11.4834(4)	11.3530(3)	11.3467(4)
b/Å	12.6000(10)	12.5663(5)	12.5145(3)	12.4786(5)	12.8172(4)	12.8308(4)
c/Å	14.4210(10)	14.3697(7)	14.3240(4)	14.2792(5)	14.1695(4)	14.1650(5)
α/deg	66.899(3)	67.016(3)	67.249(2)	67.408(2)	67.311(2)	67.291(2)
β/deg	71.281(3)	71.065(3)	70.924(2)	70.843(2)	71.185(2)	71.187(2)
γ/deg	65.383(3)	65.614(2)	65.7610(10)	65.895(2)	64.066(2)	64.040(2)
V/Å^3	1767.3(2)	1740.29(14)	1711.65(9)	1688.43(11)	1681.07(9)	1680.88(11)
d_{calc}/g cm^{-3}	1.686	1.684	1.740	1.764	1.772	1.772
θ_{max}/deg	28.060	27.969	28.539	29.677	28.585	28.697
Number of reflections						
measured	31684	23363	22503	33469	31486	27822
unique	8485	8292	8568	9319	8504	8202
(R_{int})	(0.0521)	(0.0688)	(0.1235)	(0.1791)	(0.1270)	(0.1094)
I_{hkl} ($I > 2\sigma(I)$)	4523	4603	5802	6271	6085	6085
N	613	586	559	532	478	478
GOOF	0.918	0.838	0.970	0.978	0.934	0.957
$I > 2\sigma(I)$						
R_1	0.0472	0.0620	0.0567	0.0511	0.0422	0.0367
wR_2	0.1296	0.1741	0.1491	0.1249	0.0959	0.0834
All I_{hkl}						
R_1	0.0972	0.1089	0.0813	0.0798	0.0649	0.0540
wR_2	0.1398	0.1999	0.1597	0.1470	0.1020	0.0875
CCDC	1872693	1872689	1872691	1872695	1872696	1872694

Table 5. Selected bond lengths (*d*) in solvated complexes **1**·Solv (Solv = PhH, PhMe, *o*-Xyl) at different temperatures

Bond	*d*/Å									
	1·PhH				**1**·PhMe				**1**·*o*-Xyl	
	320 K	295 K	220 K	125 K	295 K	240 K	175 K	110 K	295 K	125 K
$Cu—O_{NO}$	2.169(2)	2.150(2)	2.050(3)	1.970(1)	2.097(2)	2.066(2)	2.000(3)	1.974(3)	2.069(3)	1.979(1)
$(O_{NO})Cu—O_{hfac}$	2.181(4)	2.162(2)	2.033(5)	2.001(1)	2.073(3)	2.044(3)	2.003(3)	1.997(3)	2.059(5)	2.000(1)
$Cu—N_R$	2.012(2)	2.006(2)	2.014(4)	2.013(1)	1.999(2)	2.010(2)	2.010(3)	2.004(3)	1.996(4)	2.005(2)
$Cu—O_{hfac}$	1.968(2)	2.160(2)	1.966(4)	1.968(1)	1.959(2)	1.963(2)	1.970(3)	1.965(3)	1.954(4)	1.963(1)
	2.093(2)	1.960(2)	2.187(4)	2.255(1)	2.193(2)	2.181(2)	2.241(3)	2.257(3)	2.212(4)	2.259(1)
	2.112(2)	2.129(2)	2.237(4)	2.324(1)	2.158(2)	2.224(2)	2.301(3)	2.325(3)	2.172(4)	2.326(1)

Table 6. Selected bond lengths (*d*) in solvated complexes **2**·Solv (Solv = *o*-Xyl, *p*-Xyl) at different temperatures

Bond	*d*/Å			
	2·*o*-Xyl		**2**·*p*-Xyl	
	295 K	105 K	295 K	150 K
$Cu—O_{NO}$	2.050(3)	1.951(6)—1.974(7)	1.997(1)	1.967(1)
$(O_{NO})Cu—O_{hfac}$	2.032(4)	1.979(6)—2.025(9)	2.004(2)	1.992(1)
$Cu—N_R$	2.005(3)	1.971(6)—2.027(5)	2.005(2)	2.014(1)
$Cu—O_{hfac}$	1.955(3)	1.936(7)—1.986(5)	1.961(2)	1.968(1)
	2.184(3)		2.237(2)	2.260(1)
	2.223(3)	2.219(5)—2.368(5)	2.301(2)	2.340(1)

Table 7. Selected bond lengths (*d*) in systems **2**·Solv (Solv = PhH, PhMe, and PhBr) at different temperatures

Bond	*d*/Å					
	2·PhH					
	295 K	240 K	200 K	125 K		
$Cu—O_{NO}$	2.201(2)	2.076(1)	2.010(1)	1.985(1)		
$(O_{NO})Cu—O_{hfac}$	2.243(2)	2.220(1)	2.037(2)	2.029(1)		
$Cu—N_R$	2.002(2)	2.003(1)	1.999(2)	2.004(1)		
$Cu—O_{hfac}$	1.968(2)	1.963(1)	1.960(2)	1.967(1)		
	2.088(2)	2.09(2)	2.270(2)	2.286(1)		
	2.080(2)	2.205(2)	2.287(2)	2.311(1)		
	2·PhMe					
	295 K	240 K	200 K	150 K	105 K	
$Cu—O_{NO}$	2.321(1)	2.312(1)	2.2964(1)	2.043(2)	1.995(1)	
$(O_{NO})Cu—O_{hfac}$	2.338(2)	2.338(2)	2.331(2)	2.047(2)	2.028(2)	
$Cu—N_R$	2.010(2)	2.012(2)	2.011(2)	2.012(2)	2.012(2)	
$Cu—O_{hfac}$	1.984(2)	1.982(2)	1.982(1)	1.964(2)	1.961(1)	
	2.003(2)	2.006(2)	2.010(2)	2.263(2)	2.313(2)	
	2.009(2)	2.006(2)	2.011(2)	2.267(2)	2.317(2)	
	2·PhBr					
	295 K	240 K	175 K	115 K	95 K	91 K
$Cu—O_{NO}$	2.356(2)	2.347(3)	2.337(2)	2.326(3)	2.001(1)	1.992(1)
$(O_{NO})Cu—O_{hfac}$	2.335(3)	2.320(3)	2.332(3)	2.333(3)	2.030(26)	2.028(1)
$Cu—N_R$	2.013(2)	2.014(3)	2.015(2)	2.013(2)	2.008(2)	2.012(2)
$Cu—O_{hfac}$	1.983(2)	1.978(3)	1.976(2)	1.991(2)	1.965(2)	1.967(1)
	1.984(2)	1.983(3)	1.977(2)	1.971(2)	2.274(2)	2.280(2)
	1.986(2)	1.988(3)	1.990(2)	1.971(2)	2.304(2)	2.308(2)

lamellar crystals that formed were filtered off, washed with cold hexane, and dried on the filter in air stream. The yield was 42 mg (75%). Found (%): C, 42.4; H, 3.1; F, 28.4; N, 5.4. $C_{54}H_{50}Cu_2F_{24}N_6O_{12}$. Calculated (%): C, 41.7; H, 3.2; F, 29.3; N, 5.4.

Complexes $[Cu(hfac)_2L^{Et}]_2 \cdot PhMe$, $[Cu(hfac)_2L^{Et}]_2 \cdot o$-Xyl, $[Cu(hfac)_2L^{Et}]_2 \cdot p$-Xyl, and $[Cu(hfac)_2L^{Et}]_2 \cdot PhBr$ were obtained analogously using toluene, *o*-xylene, *p*-xylene, and bromobenzene as solvent, respectively.

Tetrakis(1,1,1,5,5,5-hexafluoro-2,4-pentanedionato-*O,O′*)-bis[μ$_2$-2-(4-ethylpydin-3-yl)-4,4,5,5-tetramethyl-4,5-dihydro-1*H*-imidazole-3-oxide-1-oxyl]dicopper(II) toluene solvate, $[Cu(hfac)_2L^{Et}]_2 \cdot PhMe$, from this point on **2 · PhMe**, yield 60%, bulky dark-red prismatic crystals. Found (%): C, 41.4; H, 3.4; F, 26.5; N, 6.0. $C_{55}H_{52}Cu_2F_{24}N_6O_{12}$. Calculated (%): C, 42.1; H, 3.3; F, 29.0; N, 5.4. Crystallization of this compound also gave a few dark-red crystals of the composition $[Cu(hfac)_2L^{Et}]_2 \cdot 3PhMe$. An X-ray study of these crystals revealed the absence of fundamental differences between the structures of molecules of this complex and $[Cu(hfac)_2L^{Et}]_2 \cdot PhMe$. Crystallographic data for $[Cu(hfac)_2L^{Et}]_2 \cdot 3PhMe$ are listed in Table 8.

Tetrakis(1,1,1,5,5,5-hexafluoro-2,4-pentanedionato-*O,O′*)-bis[μ$_2$-2-(4-ethylpydin-3-yl)-4,4,5,5-tetramethyl-4,5-dihydro-1*H*-imidazole-3-oxide-1-oxyl]dicopper(II) *o*-xylene solvate, $[Cu(hfac)_2L^{Et}]_2 \cdot o$-Xyl, from this point on **2 · *o*-Xyl**, yield 65%, dark-red needle-shaped crystals. Found (%): C, 41.7; H, 3.2; F, 26.8; N, 5.2. $C_{56}H_{54}Cu_2F_{24}N_6O_{12}$. Calculated (%): C, 42.4; H, 3.4; F, 28.8; N, 5.3.

Tetrakis(1,1,1,5,5,5-hexafluoro-2,4-pentanedionato-*O,O′*)-bis[μ$_2$-2-(4-ethylpydin-3-yl)-4,4,5,5-tetramethyl-4,5-dihydro-1*H*-imidazole-3-oxide-1-oxyl]dicopper(II) *p*-xylene solvate, $[Cu(hfac)_2L^{Et}]_2 \cdot p$-Xyl, from this point on **2 · *p*-Xyl**, yield 65%, dark-red needle-shaped crystals. Found (%): C, 40.5; H, 3.4; F, 25.3; N, 4.5. $C_{56}H_{54}Cu_2F_{24}N_6O_{12}$. Calculated (%): C, 42.4; H, 3.4; F, 28.8; N, 5.3.

Tetrakis(1,1,1,5,5,5-hexafluoro-2,4-pentanedionato-*O,O′*)-bis[μ$_2$-2-(4-methylpyridin-3-yl)-4,4,5,5-tetramethyl-4,5-dihydro-1*H*-imidazole-3-oxide-1-oxyl]dicopper(II) bromobenzene solvate, $[Cu(hfac)_2L^{Et}]_2 \cdot PhBr$, from this point on **2 · PhBr**, yield 90%, bulky black prismatic crystals. Found (%): C, 36.9; H, 2.8; Br, 8.3; F, 26.5; N, 4.4. $C_{60}H_{54}Br_2Cu_2F_{24}N_6O_{12}$. Calculated (%): C, 40.2; H, 2.9; Br, 8.9; F, 25.4; N, 4.7.

Results and Discussion

Nitroxide L^{Et} was obtained from 4-ethylnicotinaldehyde using a procedure similar to the synthesis of L^{Me}.[9] The general scheme describing the synthesis of these nitronyl nitroxide radicals is given below (Scheme 1).

We succeeded to isolate single crystals of radical L^{Et} and to study its molecular and crystal structure (Fig. 1, *a*). In the solid state, there are three crystallographically independent L^{Et} molecules with slightly different structures. In all of them, the N—O distances lie between 1.275(2) and 1.285(1) Å, which is typical of nitroxide radicals. The angles between the planes of the nitronyl nitroxide fragment CN_2O_2 and the pyridine ring (Py) in these molecules have similar values and lie in the range of ~68—74°, which is much larger than that in the corresponding nitronyl nitroxide radicals without alkyl substituents in the pyridine

Table 8. Crystallographic data for solvated complex **2 · PhMe**

Parameter	Value	
T/K	296	115
Cu-Kα/Å	1.54018	1.54018
Crystal system	Triclinic	Triclinic
Space group	$P\bar{1}$	$P\bar{1}$
a/Å	15.2084(5)	15.0670(4)
b/Å	16.1032(6)	15.9231(4)
c/Å	17.8553(6)	17.6814(5)
α/deg	81.2174(15)	81.3843(11)
β/deg	88.0213(16)	88.2391(11)
γ/deg	69.5869(15)	69.6133(10)
V/Å^3	4049.3(2)	3930.37(18)
Z	2	2
d_{calc}/g cm^{-3}	1.475	1.520
θ_{max}/deg	67.706	67.762
Number of reflections		
measured	69198	67930
unique	14454	13669
(R_{int})	(0.0638)	(0.0310)
with $I_{hkl} > 2\sigma(I)$	12318	12638
N_{par}	1216	11246
R	0.0398	0.0396
wR_2	0.1144	0.1124
GOOF	1.050	1.054
CCDC	1872688	1872701

Scheme 1

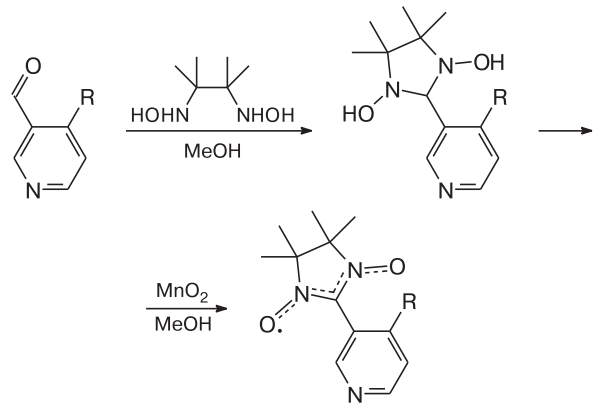

R = Me (63%), Et (40%)

ring (L^H, 35.1°) and larger than a value of 53.0° obtained for L^{Me}.[13] The shortest contacts between the nitroxide O atoms of adjacent molecules in L^{Et} are ~3.8 Å; as a consequence, there are no strong exchange interactions between the nitroxide spins (J/k = –0.70±0.01 K) and the effective magnetic moment μ_{eff} has a nearly constant value of 1.74 μ_B throughout the temperature range 30—300 K (Fig. 1, *b*). This value is in good agreement with the theoretical spin-only value 1.73 μ_B for noninteracting PMC with the spin S = 1/2 and *g*-factor *g* = 2.

Reactions between equimolar amounts of $Cu(hfac)_2$ and L^{Me} in different solvents reproducibly gave solvates **1**·PhH, **1**·PhMe, and **1**·*o*-Xyl upon crystallization from benzene, toluene, and *o*-xylene, respectively.

A study of the molecular and crystal structures of the compounds in the temperature range of 100—295 K revealed similar structural dynamics for all of them (see Table 5). The crystal structures of solvates **1**·Solv (Solv is benzene, toluene, and *o*-xylene) are composed of centrosymmetrical molecules (Fig. 2). Copper atoms are in compressed octahedral environment where axial distances are shorter than equatorial ones. The nitroxide O atom lies in the equatorial plane, the $Cu—O_{NO}$ distances being 2.150(2), 2.097(2), and 2.069(3) Å at T = 295 K. Axial positions in the complexes with Solv = PhH, PhMe, and *o*-Xyl are occupied by the O_{hfac} and N_{Py} atoms ($d_{Cu—O}$ 1.954(4)—1.960(2) Å; $d_{Cu—N}$ 1.996(4)—2.006(2) Å, see Table 5). The $Cu—O_{NO}$ and $Cu—O_{hfac}$ distances (Cu,

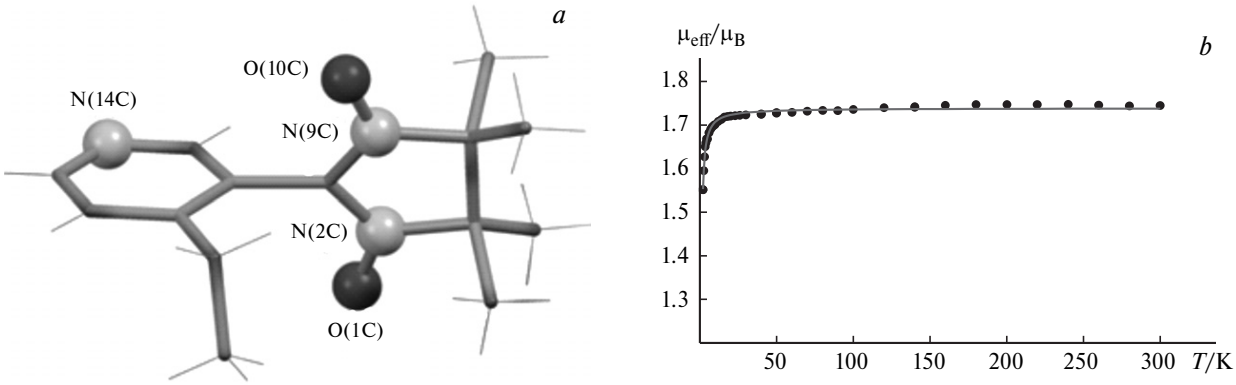

Fig. 1. Molecular structure of L^{Et} (*a*) and experimental dependence $\mu_{eff}(T)$ (*b*) for L^{Et}.

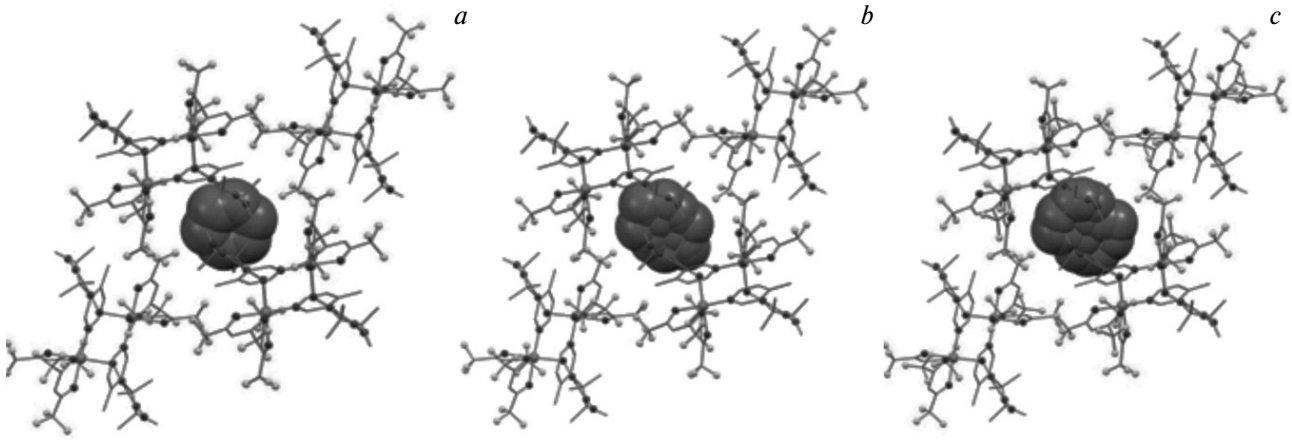

Fig. 2. Structures of complexes **1**·PhH (*a*), **1**·PhMe (*b*), and **1**·*o*-Xyl (*c*).

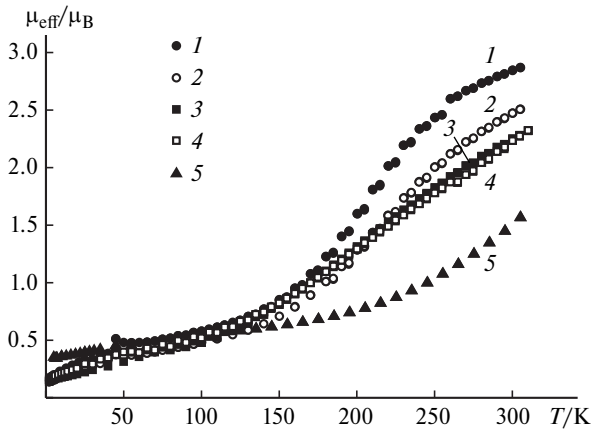

Fig. 3. Experimental dependences $\mu_{eff}(T)$ for solvates **1**•PhH (*1*), **1**•PhMe (*2*), **1**•*o*-Xyl (*3*), **2**•*o*-Xyl (*4*), and **2**•*p*-Xyl (*5*).

O_{hfac}, and O_{NO} atoms lie on the same axis) in the coordination sites decrease to 1.970(1)—1.979(1) and 1.954(1)—1.968(1) Å, respectively, upon cooling to 100 K (see Table 5). In all the three complexes the solvent molecules are located in identical cavities (see Fig. 2).

The experimental dependences $\mu_{eff}(T)$ obtained for complexes **1**•Solv (Solv = PhH, PhMe, *o*-Xyl) are similar (Fig. 3). At room temperature, the μ_{eff} value is in the range of about 2.87—2.33 μ_B, which is smaller than the theoretical spin-only value 3.46 μ_B for four PMC with S = 1/2 and *g* = 2. This suggests that spin transitions do occur at room temperature. The μ_{eff} value gradually decreases to ~0.2 μ_B on cooling, thus indicating an almost complete spin pairing. The magnetochemical data are in good agreement with the X-ray diffraction data on the structural rearrangement followed by significant shortening of the $Cu—O_{NO}$ distances. This is accompanied by the onset of strong antiferromagnetic interactions in the exchange clusters {>N—˙O—Cu^{2+}}, which leads to spin compensation for PMC.[14]

The reaction of $Cu(hfac)_2$ with L^{Et} also gave centrosymmetrical dinuclear complexes with solvate molecules in the packing. However, we isolated a wider variety of solvates as individual phases, *viz.*, complexes with benzene, toluene, bromobenzene, *o*-xylene, and *p*-xylene. The molecular packing type in the solid state of solvates **2**•*o*-Xyl and **2**•*p*-Xyl is almost identical to that of the complexes **1**•Solv described above (Fig. 4, *cf.* Fig. 2).

At 295 K in the complex molecules **2**•*o*-Xyl and **2**•*p*-Xyl the vertices of the copper square bipyramid are occupied by the O_{hfac} atoms ($d_{Cu—Ohfac}$ 2.184(3)—2.302(2) Å), the O_{NO} atoms being located in equatorial positions. The $Cu—O_{NO}$ bond lengths are equal to 2.050(3) for Solv = *o*-Xyl and 1.997(2) Å for Solv = *p*-Xyl. The distances between the Cu, O_{NO}, and O_{hfac} atoms lying on the same axis decrease upon cooling to 100 K. Namely, the $Cu—O_{NO}$ distance decreases from 2.050(3) to 1.951(6)—1.974(7) Å for Solv = *o*-Xyl and from 1.997(2) to 1.967(1) Å for Solv = *p*-Xyl. From the shape of the experimental dependences $\mu_{eff}(T)$ for solvates **2**•Solv (see Fig. 3) it follows that the spin transition in two systems, **2**•*o*-Xyl and **2**•*p*-Xyl, partially occurred at room temperature. Cooling of the samples causes the μ_{eff} values to smoothly decrease to 0.16—0.65 μ_B as a consequence of nearly complete mutual compensation of PMC spins. Thus, the results of thermomagnetic measurements are in excellent agreement with the X-ray diffraction data on the structural rearrangement of exchange clusters accompanied by considerable shortening of $Cu—O_{NO}$ distances (see Table 6).

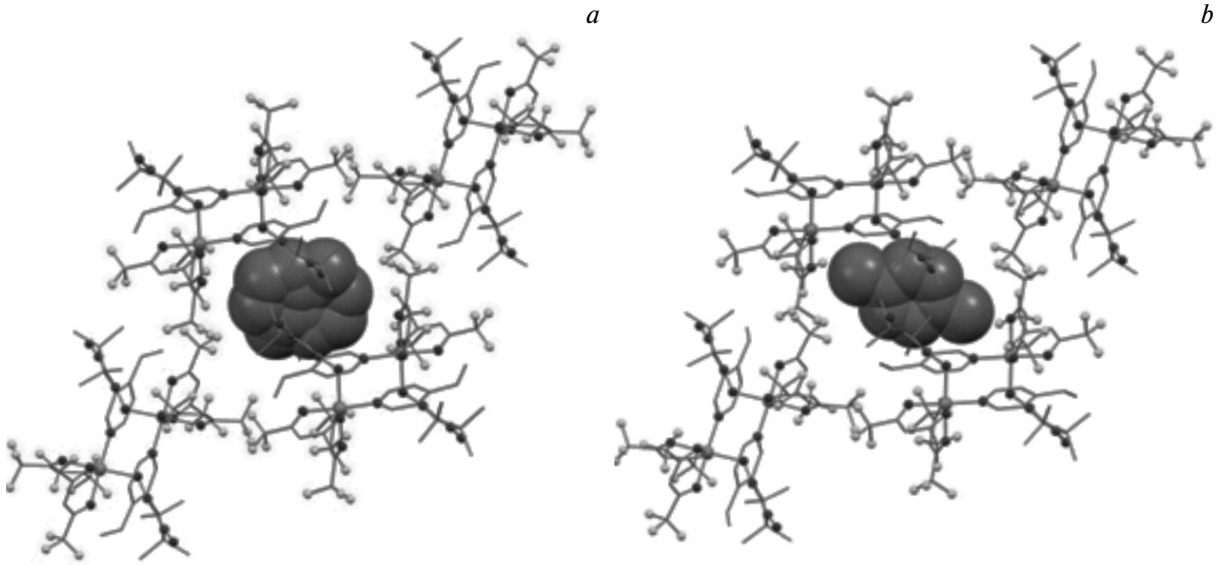

Fig. 4. Structures of complexes **2**•*o*-Xyl (*a*) and **2**•*p*-Xyl (*b*).

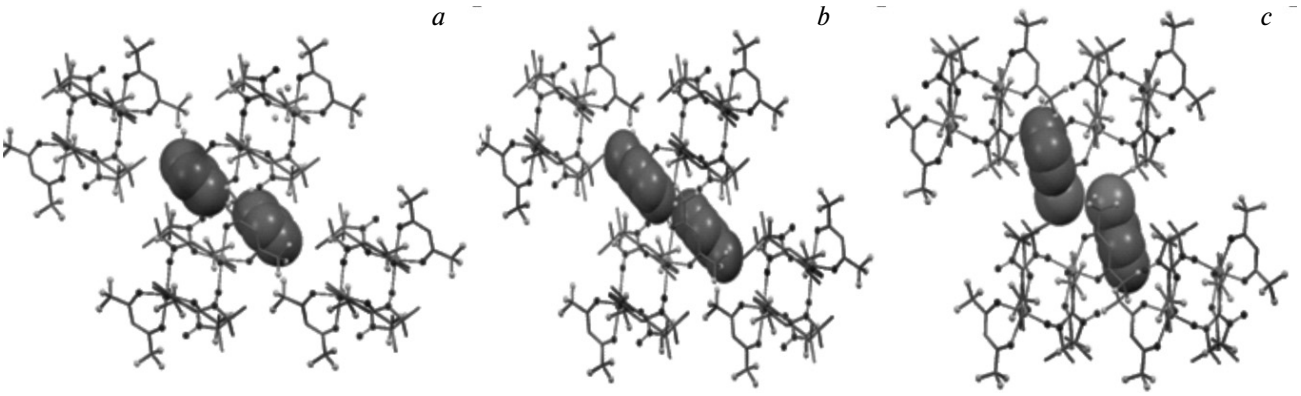

Fig. 5. Structural fragments of **2** • PhH (*a*), **2** • PhMe (*b*), and **2** • PhBr (*c*).

The solvate complexes with benzene, bromobenzene, and toluene obtained by the reaction of $Cu(hfac)_2$ with L^{Et} differ from the monoclinic crystals discussed above in lower, *viz.*, triclinic symmetry, packing type, and much longer Cu—O_{NO} distances in the coordination sites. In the complexes **2** • PhH, **2** • PhBr, and **2** • PhMe the solvent molecules occupy another type of cavities (Fig. 5) and the magnetic properties of the complexes (Fig. 6) appeared to be more sensitive to the nature of the solvent molecules.

For the complexes **2** • PhMe and **2** • PhBr one has μ_{eff} = 3.48 μ_B at 300 K, which is in good agreement with the theoretical spin-only value 3.46 μ_B for four noninteracting PMC with $S = 1/2$ and $g = 2$. As temperature decreases, μ_{eff} (**2** • PhBr) gradually increases to 3.65 μ_B at 100 K, then abruptly decreases to 1.13 μ_B at 95 K, and smoothly decreases to 0.41 μ_B at 2 K. A slight increase in μ_{eff} in the temperature range of 300—100 K is indicative of weak ferromagnetic exchange interactions between PMC spins, whereas at $T < 100$ K, one deals with almost complete mutual compensation of PMC spins owing to strong antiferromagnetic interactions. For **2** • PhMe, the μ_{eff} value varies only slightly as temperature decreases to 210 K, then rapidly decreases, and then gradually decreases at $T < 200$ K down to μ_{eff} = 0.24 μ_B at 2 K. The effective magnetic moment of complex **2** • PhH is 2.98 μ_B at 300 K, then decreases to 0.81 μ_B at 100 K as temperature decreases, and then remains almost unchanged. The value 2.98 μ_B (**2** • PhH) at 300 K is smaller than the theoretical spin-only value 3.46 μ_B for four noninteracting PMC with $S = 1/2$ and $g = 2$; thus, the spin transition occurs in the range of ambient temperatures.

The temperature dependences $\mu_{eff}(T)$ for the solvates **2** • PhH, **2** • PhMe, and **2** • PhBr are in good agreement with the X-ray diffraction data. The crystal structures of the dinuclear complexes are composed of centrosymmetrical molecules. At room temperature, Cu atoms in all solvates **2** • Solv are in identical environment, *viz.*, axial positions of the Cu bipyramid are occupied by the nitroxide O atoms ($d_{Cu—ONO}$ 2.201(2), 2.321(2), and 2.356(2) Å) and one of the O_{hfac} atoms (2.243(2), 2.338(2), and 2.335(3) Å), while equatorial positions are occupied by three O_{hfac} atoms ($d_{Cu—Ohfac}$ 1.968(2)—2.088(2) Å) and the N_{Py} atom ($d_{Cu—Npy}$ 2.002(2)—2.013(2) Å). As temperature decreases, a structural rearrangement occurs, accompanied by transition of the coordinated O_{NO} atoms from axial to equatorial positions (see Table 7); this causes the onset of strong antiferromagnetic exchange interactions and PMC spin compensation.[14] In **2** • PhH the axial Cu—O distances are ~0,1 Å shorter (see Table 7) while equatorial ones are ~0,1 Å longer than in **2** • PhMe and **2** • PhBr already at room temperature. As temperature decreases, the Cu—O_{NO} distances in complex **2** • PhH are smoothly shortened in a rather wide temperature range (see Table 7) and a smooth spin transition accompanied by a decrease in μ_{eff} occurs. Thus, by varying the nature of the solvate molecules one can induce abrupt changes in the temperature and in the character of the spin transition. In the complex with bromobenzene one deals with a sharp change from weak ferromagnetic to strong antiferromagnetic

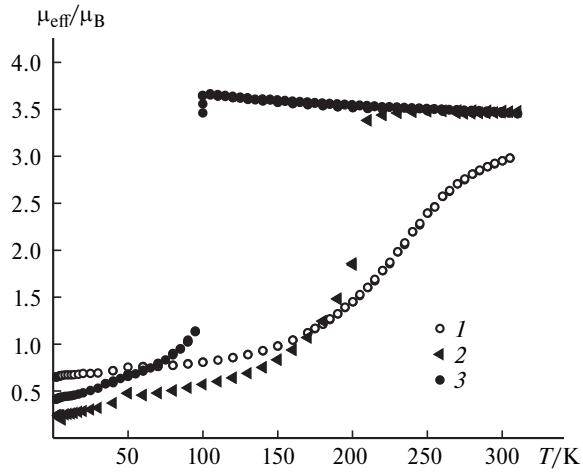

Fig. 6. Experimental dependences $\mu_{eff}(T)$ for solvates **2** • PhH (*1*), **2** • PhMe (*2*), and **2** • PhBr (*3*).

exchange interaction at $T = 100$ K, whereas for the complex with toluene the character of exchange interaction abruptly changes from weak to strong antiferromagnetic at $T = 180$ K, while for the complex with benzene a smooth spin transition begins in the range of ambient temperatures.

Comparing the results obtained in this study of molecular solvates with the data obtained earlier for the solvates of polymer chain complexes, mention may be made that the $\mu_{eff}(T)$ dependences for the crystals composed of heterospin chains are much more sensitive to the type and even orientation of solvent molecules in the interchain space than the parameters of the spin transitions of the heterospin molecular solvates that are primarily sensitive only to the change in the crystal packing type. In fact, heterospin chains can act as sensors for particular type of solvent molecules (provided that the general structural motif for the mutual arrangement of chains remains unchanged), whereas in molecular crystals the magnetic properties of the multispin compounds are sensitive to the change in the packing type rather than to the nature of the solvate molecules.

This work was financially supported by the Russian Foundation for Basic Research (Project Nos 18-33-00491 and 18-29-04002 — magnetic measurements), the Council on Grants at the President of the Russian Federation (Grant MK-1970.2018.3, synthesis), and by the Russian Science Foundation (Project No. 17-13-01022, low-temperature X-ray diffraction study).

References

1. V. A. Morozov, R. Z. Sagdeev, *Russ. Chem. Bull.*, 2017, **66**, 201.
2. M. Swart, M. Costas, *Spin States in Biochemistry and Inorganic Chemistry*, J. Wiley & Sons, 2016.
3. V. I. Ovcharenko, E. G. Bagryanskaya, in *Spin-Crossover Materials: Properties and Applications*, Ed. M. Halcrow, J. Wiley & Sons, 2013, p. 239.
4. P. Rey, V. I. Ovcharenko, in *Magnetism: Molecules to Materials, IV*, Eds J. S. Miller, M. Drillon, Wiley-VCH, New York, 2003, 41.
5. V. I. Ovcharenko, in *Stable Radicals: Fundamentals and Applied Aspects of Odd-Electron Compounds*, Ed. R. Hicks, Wiley-VCH, New York, 2010, 461.
6. V. I. Ovcharenko, G. V. Romanenko, K. Yu. Maryunina, A. S. Bogomyakov, E. V. Gorelik, *Inorg. Chem.*, 2008, **47**, 9537.
7. G. V. Romanenko, K. Yu. Maryunina, A. S. Bogomyakov, R. Z. Sagdeev, V. I. Ovcharenko, *Inorg. Chem.*, 2011, **50**, 6597.
8. K. Yu. Maryunina, G. V. Romanenko, E. M. Zueva, S. V. Fokin, A. S. Bogomyakov, V. I. Ovcharenko, *Russ. Chem. Bull.*, 2013, **62**, 2337.
9. S. E. Tolstikov, N. A. Artiukhova, G. V. Romanenko, A. S. Bogomyakov, E. M. Zueva, I. Yu. Barskaya, M. V. Fedin, K. Yu. Maryunina, E. V. Tretyakov, R. Z. Sagdeev, V. I. Ovcharenko, *Polyhedron*, 2015, **100**, 132.
10. Pat. EP2266562A1. France, 2010, 59 p.
11. V. I. Ovcharenko, S. V. Fokin, G. V. Romanenko, I. V. Korobkov, P. Rey, *Russ. Chem. Bull.* 1999, **48**, 1519.
12. J. A. Bertrand, R. I. Kaplan, *Inorg. Chem.*, 1966, **5**, 489.
13. Cambridge Structural Database, Version 5.39, Cambridge Crystallographic Data Center, Cambridge, November 2017 (last update August 2018).
14. R. N. Musin, P. V. Schastnev, S. A. Malinovskaya, *Inorg. Chem.*, 1992, **31**, 4118.

Received October 16, 2018;
in revised form January 9, 2019;
accepted January 24, 2019